

# Phase transitions and multicritical behavior in the Ising model with dipolar interactions

M. A. Bab,<sup>\*</sup> C. M. Horowitz, M. L. Rubio Puzzo, and G. P. Saracco

*Instituto de Investigaciones Físicoquímicas Teóricas y Aplicadas, CONICET, Facultad de Ciencias Exactas Universidad Nacional de La Plata, Sucursal 4, CC 16(1900) La Plata, Argentina*

(Received 2 August 2016; published 4 October 2016)

In this work, the phase diagram of the ferromagnetic Ising model with dipole interactions is revisited with the aim of determining the nature of the phase transition between stripe-ordered phases with width  $n$  ( $h_n$ ) and tetragonal liquid (TL) phases. Extensive Monte Carlo simulations are performed in order to study the short-time dynamic behavior of the observables for selected values of the ratio between the ferromagnetic exchange and dipolar constants  $\delta$ . The obtained results indicate that the  $h_1$ -TL phase transition line is continuous up to  $\delta = 1.2585$ , while for the  $h_2$ -TL line a weak first-order character is found in the interval  $1.2585 \leq \delta \leq 1.36$  and becomes continuous for  $1.37 \leq \delta \leq 1.9$ . This result suggests the existence of a tricritical point close to  $\delta = 1.37$ . When it is appropriate, the complete set of critical exponents is obtained, and in all the studied cases they depend on  $\delta$  but do not belong to the Ising universality class. Furthermore, short-time dynamic studies reveal that at the point where the mentioned lines meet the  $h_1$ - $h_2$  line, i.e., at  $\delta = 1.2585$ , the critical phase corresponding to the  $h_1$ -TL transition coexists with the  $h_2$  phase.

DOI: [10.1103/PhysRevE.94.042104](https://doi.org/10.1103/PhysRevE.94.042104)

## I. INTRODUCTION

The two-dimensional Ising model with short-range ferromagnetic exchange and long-range antiferromagnetic dipole interactions has been extensively investigated in recent decades. In spite of its simplicity, the competition between the exchange and dipole interactions, which creates frustration, originates an interesting but complex behavior. In particular, attention has been focused on the phase diagram since both theoretical [1–3] and numerical studies [1,4–7] have contributed to explaining a variety of experimentally observed structures in anisotropic ultrathin magnetic films, for example, stripe domain patterns [8–11]. The dimensionless Hamiltonian of the model is written as

$$\mathcal{H} = -\delta \sum_{\langle i,j \rangle} \sigma_i \sigma_j + \sum_{i < j} \frac{\sigma_i \sigma_j}{r_{ij}^3}, \quad (1)$$

where  $\sigma_i = \pm 1$  is the Ising spin variable oriented perpendicularly to the square lattice of size  $L$  and  $\delta = J/g$  is the ratio between the short-range ferromagnetic exchange constant  $J > 0$  and the long-range antiferromagnetic dipole coupling constant  $g > 0$ . The first sum runs over all pairs of nearest-neighbor (NN) spins, while the second one runs over all pairs of spins  $(i, j)$  of the lattice separated by a distance  $r_{ij}$ , measured in crystal units.

By using theoretical arguments, the pioneering work of Taylor, MacIsaac, and coauthors has contributed significantly to determining the phases exhibited by the model [1–3]. In this way, MacIsaac *et al.* have shown that for  $\delta < 0.425$  the ground state is antiferromagnetic (AF), while for  $\delta > 0.425$  stripe spin configurations with opposite magnetization running along one axis of the lattice are observed. These phases are characterized by an integer width  $h$  fixed all over the lattice, which increases with  $\delta$ .

On the other hand, from the Monte Carlo (MC) simulations on square lattices, it was possible to access the phase diagram in the  $T$ - $\delta$  plane, where  $T$  is the temperature of the thermal

bath [1,4–7]. At low temperatures, the model still presents AF configurations in the range  $0 < \delta < 0.4152$ , and this phase changes to irregular checkerboard configurations (IRC) with rectangular spin domains in the narrow range  $0.4152 < \delta < 0.4403$  [4]. For larger values of  $\delta$ , the system state is characterized by the same stripe configurations found in the ground state. Extensive studies of staggered magnetization [6,12,13] have shown that the transition lines between the described phases (IRC- $h_1$ ,  $h_1$ - $h_2$ ,  $h_2$ - $h_3$ , and so on, where  $h_n$  means  $h = n$ ) have a first-order character. In particular, the  $h_1$ - $h_2$  transition was found at  $\delta = 1.2585$  [6].

At higher temperatures all the phases change to disordered states characterized by a fourfold discrete rotational symmetry [14], called tetragonal liquid (TL), except for narrow windows around  $\delta = 2.2$  and  $\delta = 2.8$ , where intermediate nematic phases, between stripes and TL phases, were observed [6,7]. Finally, with a further temperature increase, the tetragonal fourfold symmetry is continuously replaced by the full-rotational symmetry corresponding to the paramagnetic phase [8].

The continuous character of the AF-TL phase transition line was determined by studying the thermal evolution of the specific heat [5]. However, for the IRC-TL transition a first-order line was reported, and the existence of a tricritical point was suggested, although these facts are not completely clear [5]. In the case of the transition between stripes and TL phases, it was stated recently that the phase transition  $h_1$ -TL is continuous up to  $\delta = 1.2$ . This puts an end to a long-standing controversy about the order of this transition line [15,16]. Furthermore, a full characterization of the critical behavior along this line up to  $\delta = 1.2$  was also given [16]. On the other hand, both works have reported a first-order transition for  $\delta = 1.3$  that corresponds to the  $h_2$ -TL transition, in agreement with previous results [6]. This fact may suggest the existence of a multicritical point somewhere in the interval  $1.2 < \delta < 1.3$ . It is important to mention that these findings were obtained by using two quite different techniques: (a) the analysis of the complex partition function zeros from multicanonical algorithms [15] and (b) the study of the dynamic evolution of the order parameter and its moments at the early stages

<sup>\*</sup>mbab@inifta.unlp.edu.ar

of its evolution, named short-time dynamics (STD) [16]. In addition, Rastelli *et al.* [4,5] have given evidence that first-order transitions occur at  $\delta = 1.7$  and  $2.5$ , i.e.,  $h_2$ -TL and  $h_3$ -TL, respectively. Nevertheless, a full characterization of the transition lines for  $h_n$ -TL for  $n \geq 2$  is still necessary.

The difficulties in the characterization of the transition lines are, on the one hand, a consequence of the difficulties introduced in the simulations due to the presence of long-range dipole interactions, such as an important increase in the simulation times that limits the system size used and strong finite-size effects. On the other hand, they are due to the existence of multiple metastable states at low temperatures and weak first-order phase transitions [6]. As a consequence, any convincing finite-size scaling is hindered.

In this context, the STD method has proven to be a powerful technique to avoid these hindrances, displaying its ability to determine the nature of the  $h_1$ -TL transition [16]. In fact, STD studies are performed by considering the early time evolution of the relevant observables, before reaching equilibrium states. This means a huge reduction in computational time. Moreover, due to the fact that the finite-size effects do not significantly affect the dynamic evolution of the observables within the short-time regime, the results could be attributed to those corresponding to the thermodynamic limit, avoiding the finite-size analysis. Furthermore, STD has been successfully applied to several models in order to differentiate a weak first-order phase transition from a continuous one and to study the multicritical behavior. For more information about the application of STD, see the recent report of Albano *et al.* [17] and references therein.

In this work the transition lines between stripes and TL phases are studied in the interval  $1.2 < \delta < 2$  by means of the STD method. The aim is to determine the order of the transitions as a function of  $\delta$ , to characterize the critical behavior in the case of the continuous transition, and from the results to determine the existence of multicritical points. This paper is organized as follows: in Sec. II the simulation details and a summary of the STD method are given, and in Sec. III the results are presented and discussed. Finally, the conclusions are reported in Sec. IV.

## II. SHORT-TIME DYNAMICS AND SIMULATION DETAILS

As was mentioned, the dynamic behavior of the Ising model with dipolar interactions will be studied by employing the STD. This method consists of the analysis of the dynamic evolution of some observables in a neighborhood of the transition points for different values of the control parameter, in the present case the temperature. The observables are typically the order parameter  $O_p$ , its second moment  $O_p^2$ , the susceptibility  $\chi$ , the logarithmic derivative of  $O_p$  with respect to the reduced temperature  $D$  evaluated at the critical point  $T_c$ , and the second-order Binder cumulant  $U$ .

For our purposes, the order parameter has to be sensitive to the change in the orientational order, such as the one introduced by Booth *et al.* [14],

$$O_p \equiv O_{hv} \equiv \frac{n_v - n_h}{n_v + n_h}, \quad (2)$$

where  $n_v$  ( $n_h$ ) is the number of vertical (horizontal) bonds of the NN antiparallel spins. This definition ensures that  $O_p =$

$+1$  ( $-1$ ) when the system is in the stripe horizontal (vertical) phase and  $O_p = 0$  in the TL or paramagnetic phase. Due to the fact that  $O_{hv}$  does not distinguish between  $h_n$  and  $h_{n+1}$  phases, it is necessary to modify the definition (2) in order to take into account the effects of the proximity of the first-order transition  $h_1$ - $h_2$ . This topic will be discussed in detail in the following section. Nevertheless, the other observables can be defined in a general way:

$$\chi = \frac{1}{N} (\langle O_p^2 \rangle - \langle O_p \rangle^2), \quad (3)$$

$$D \equiv \left. \frac{\partial \log \langle O_p \rangle}{\partial \tau} \right|_{\tau=0}, \quad (4)$$

$$U = 1 - \frac{\langle O_p^2 \rangle}{\langle O_p \rangle^2}, \quad (5)$$

where  $\tau = (T - T_c)/T_c$  is the reduced temperature,  $N = L^2$ , and  $\langle \dots \rangle$  indicates the average performed over different realizations from equivalent initial conditions. Hereafter,  $\langle O_p \rangle$  and  $\langle O_p^2 \rangle$  will be referred to as  $O_p$  and  $O_p^2$ , respectively.

The dynamic evolution of the observables is measured when the system is initialized from configurations corresponding to the trivial fixed points [17], i.e., the ground state at  $T = 0$  and the paramagnetic one at  $T = \infty$ . In the case of a continuous phase transition, it is expected that the observables defined above will exhibit a power-law behavior at the critical point within the short-time regime, with exponents related to the critical exponents of the phase transition. For values of the control parameter  $T \neq T_c$ , but at the criticality, the power law is modified by a scaling function. This fact allows us to determine the critical temperature as well as the critical exponents from the localization of the best power law (for more details, see the review in Ref. [17] and references therein).

For the case of the ground-state initial condition, the *Ansatz* of the time evolution of the observables are the following:

$$O_p(t) \propto t^{-\beta/\nu z}, \quad (6)$$

$$\chi(t) \propto t^{\gamma/\nu z}, \quad (7)$$

$$U(t) \propto t^{d/z}, \quad (8)$$

$$D(t) \propto t^{1/\nu z}, \quad (9)$$

where  $\beta, \nu$ , and  $\gamma$  are the static exponents for the order parameter, correlation length, and susceptibility, respectively, and  $z$  is the dynamic exponent for the time evolution of the spatial correlation length.

However, if the system is started from paramagnetic initial condition, the proposed scaling law is

$$O_p^2(t) = \chi(t) \propto t^{\gamma/\nu z}. \quad (10)$$

It is important to mention that the universal evolution is strictly valid in a well-defined time interval  $(t_{\text{mic}}, t_{\text{max}})$ , where  $t_{\text{mic}}$  and  $t_{\text{max}}$  are set when the spatial correlation length  $\xi(t)$  is of the order of a single lattice spacing and the lattice size  $L$ , respectively. Furthermore, STD is free of the critical slowing down due to the fact that  $t_{\text{max}}$  is smaller than the equilibration

time. It is well known that for short-range models, STD is free of finite-size effects since  $\xi(t) \ll L$ , but this is no longer valid for long-range models. In fact, it was observed that the cutoff introduced in the interaction sum, when periodic boundary conditions are implemented, affects the validity range of the power-law behavior but not the corresponding exponents [18].

In addition, STD can also be applied to determine the metastability limits of the coexisting phases in a first-order phase transition [17,19]. At these points the susceptibility and relaxation times diverge, as in the case of a continuous phase transition. This fact allows us to define them as pseudocritical points and identify them as the spinodals. In this way, for the ground-state initial condition the  $O_p$  behaves as

$$O_p(t) \propto t^\omega + O_p^{sp}, \quad (11)$$

where  $\omega$  is an exponent and  $O_p^{sp}$  is the value of the order parameter at the spinodal point  $T_{up}$ . Also, the susceptibility diverges as a power law given by

$$\chi(t) \propto t^\Omega, \quad (12)$$

where  $\Omega$  is an exponent. For the paramagnetic initial condition  $O_p^2$  is given by

$$O_p(t)^2 \propto t^{\omega^*}, \quad (13)$$

where  $\omega^*$  is another exponent, and  $O_p^{sp} = 0$  at the other spinodal  $T_{down}$ . The difference  $T_{up} - T_{down}$  is a measure of the strength of the transition, and it allows us to distinguish between a continuous transition, where  $T_{up} = T_{down} = T_c$ , and a weak first-order transition ( $T_{down} < T_{trans} < T_{up}$ , where  $T_{trans}$  is the transition temperature [17]).

In order to properly treat the effects of the above-mentioned cutoff, periodic boundary conditions were set in such a way that the entire space is tiled with replicas of the original finite system. The original system and its replicas called the aggregation and are represented by the pairs  $(L, m)$ , where  $m$  is the size of the aggregation in units of replicas. In this way, the Hamiltonian in Eq. (1) is replaced by an Ising-type Hamiltonian, with effective interaction coefficients that take into account not only the interactions of the original system but also the interactions with its replicas [16,20]. This method is a simpler and alternative way to the Ewald summation techniques [21]. In previous work, it was checked that  $m \sim 5000$  is enough to reproduce the results reported by other authors. More details about these methods can be found in Refs. [16,20].

Monte Carlo simulations (MCS) were performed in a square lattice with size  $L = 128$  using periodic boundary conditions with aggregation size  $m = 5000$ . The STD observables were measured until 3000 MCS were performed and averaged over 3000 different realizations. The time interval that defines the range of validity of STD scaling was determined as  $t_{mic} \approx 100$  MCS and  $t_{mac} > 3000$  MCS.

### III. RESULTS AND DISCUSSION

#### A. Phase transitions at $\delta = 1.2585$

In order to report the obtained results, let us start from the point  $\delta = 1.2585$ . As has been mentioned, at this  $\delta$  value a first-order phase transition line between the ordered phases

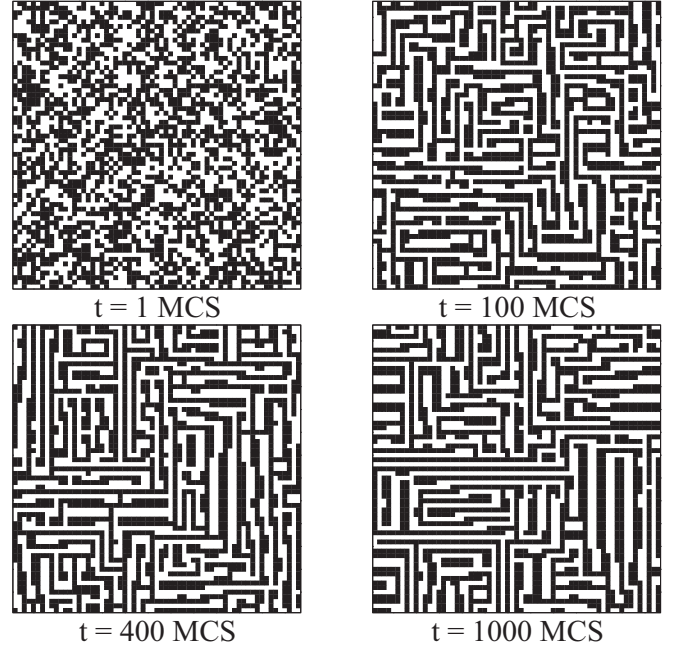


FIG. 1. Dynamic evolution of the system at  $\delta = 1.2585$  and  $T = 0.226$ , when it is started from DC. Up (down) spins are indicated with black (white) squares. The evolution times are indicated below each configuration.

$h_1$ - $h_2$  extends from  $T = 0$  up to a temperature where the order-TL transition takes place. As a consequence, the phase coexistence leads to the observation of metastable phases around the whole line. So it is reasonable to think that this fact will affect the dynamic observables in such a way that may lead to misinterpretations of the results. Furthermore, the nature of the order-TL transition point is uncertain, and it has been conjectured to be a triple [6] or tricritical point [15], where the three involved phases coexist or become critical, respectively.

Figure 1 illustrates the time evolution of the system from the initial paramagnetic state by means of a series of snapshots taken at  $\delta = 1.2585$  and  $T = 0.226$ . As can be observed,  $h_1$  and  $h_2$  domains start to grow inside the bulk of the TL phase. It is evident that the measurement of  $O_{hv}$  will be affected by this behavior, so the order parameter definition Eq. (2) must be modified in order to detect an order-disorder phase transition with a specific ordered structure, either  $h_1$  or  $h_2$ . For this reason, it is necessary to introduce two new order parameters. On the one hand, an order parameter sensitive to the phase transition between the  $h_1$  and TL phases is defined as

$$O_{hv_1} \equiv \frac{n_{v_1} - n_{h_1}}{n_v + n_h}, \quad (14)$$

where now  $n_{v_1}$  ( $n_{h_1}$ ) is the number of spins that have vertical (horizontal) antiparallel NN; that is,  $O_{hv_1}$  detects configurations of the sequence  $(-\sigma_{\mathbf{u}-\epsilon})(\sigma_{\mathbf{u}})(-\sigma_{\mathbf{u}+\epsilon})$ , where  $\sigma_{\mathbf{u}}$  is the value of the spin in the lattice position  $\mathbf{u} = (i, j)$  and  $\epsilon = (1, 0)$  or  $(0, 1)$ . Furthermore,  $n_v$  ( $n_h$ ) is the number of vertical (horizontal) bonds of the NN antiparallel spins, already defined in Sec. II.

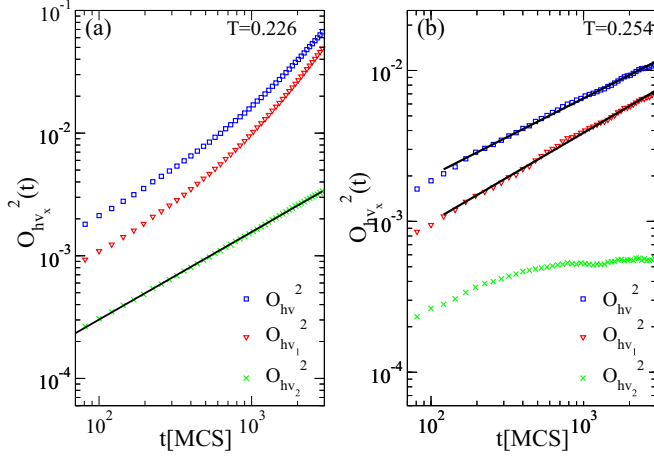


FIG. 2. Dynamic evolution of  $O_{hv}^2$ ,  $O_{hv_1}^2$ , and  $O_{hv_2}^2$  at  $\delta = 1.2585$  when the system is started from DC at the temperatures (a)  $T = 0.226$  and (b)  $T = 0.254$ . The power-law fits are indicated with a solid line. More details are given in the text.

On the other hand, the order parameter that detects the  $h_2$ -TL phase transition is defined as

$$O_{hv_2} \equiv \frac{n_{v_2} - n_{h_2}}{2(n_v + n_h)}, \quad (15)$$

where  $n_{v_2}$  ( $n_{h_2}$ ) is the number of spins in the vertical (horizontal) direction, whose NN are antiparallel between them; that is, the sequence in this case is  $(-\sigma_{u-\epsilon})(\sigma_u)(\sigma_{u+\epsilon})$ . Here the factor 2 must be added since this sequence is repeated twice.

The definition (14) ensures that  $O_{hv_1} = 1$  ( $-1$ ) when the system is in the stripe-ordered horizontal (vertical) phase  $h_1$  or  $O_{hv_1} = 0$  in the TL, paramagnetic, and  $h_2$  phases. Equivalently,  $O_{hv_2}$  is nonzero in the  $h_2$  phase, and it becomes null in the TL, paramagnetic, and  $h_1$  phases.

It is important to mention that all the expressions enumerated in Sec. II remain valid for both defined order parameters. Also, the dynamic behavior of  $O_{hv_1}$  and  $O_{hv_2}$  matches that corresponding to  $O_{hv}$  far from the  $h_1$ - $h_2$  line, as will be discussed below.

Figure 2 shows the time evolution of the  $O_{hv}^2$ ,  $O_{hv_1}^2$ , and  $O_{hv_2}^2$  from the initial disordered configurations (DC) at the indicated temperatures. For  $O_{hv_2}^2$  the power-law behavior is evident at  $T = 0.226$ , while  $O_{hv_1}^2$  and  $O_{hv}^2$  present upward deviations [see Fig. 2(a)]. On the other hand, Fig. 2(b) shows that  $O_{hv_1}^2$  and  $O_{hv}^2$  exhibit a similar power-law behavior at  $T = 0.254$ , while  $O_{hv_2}^2$  quickly saturates at a small value. This result can be understood due to the fact that there are, on average, tiny structures of  $h = 2$  at this temperature, but its contribution to  $O_{hv}$  dynamic behavior is not significant.

The presence of the above-mentioned first-order transition line makes the ground state twofold. In fact, there are two possible initial ground-state configurations at  $\delta = 1.2585$ , i.e., the ordered configurations  $h_1$  and  $h_2$ . These initial configurations have to be considered if the  $h_1$ -TL or  $h_2$ -TL transitions are studied by means of the STD method.

Figure 3 exhibits the dynamic behavior of  $O_{hv}$ ,  $O_{hv_1}$ , and  $O_{hv_2}$  as well as the corresponding susceptibility  $\chi$ . In order to study the phase transition  $h_1$ -TL, the system was started

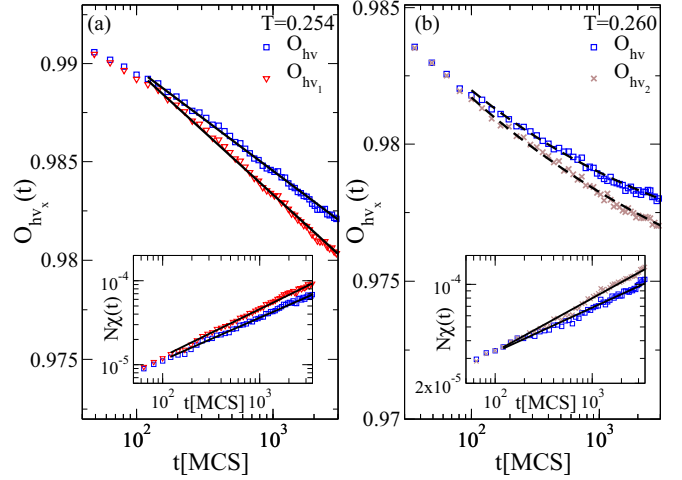


FIG. 3. Dynamic evolution of (a)  $O_{hv}$  and  $O_{hv_1}$  at  $\delta = 1.2585$  when the system is started from the  $h_1$  OC at the temperature  $T = 0.254$  and (b)  $O_{hv}$  and  $O_{hv_2}$  when the system is started from the  $h_2$  OC at the temperature  $T = 0.260$ . The insets show the evolution of the susceptibilities that exhibit power-law behavior at these temperatures. The solid lines correspond to the fits using the STD equations. More details are given in the text.

from the ordered configuration (OC) with the  $h_1$  configuration. Figure 3(a) indicates that the power-law behavior of  $O_{hv_1}$ , according to Eq. (6), is found at  $T = 0.254$ , i.e., at the same temperature obtained for the DC case [see Fig. 2(b)]. Note that  $O_{hv}$  presents a slightly different power-law behavior at this temperature due to the fact that the definition of  $O_{hv_1}$  only takes into account domains with stripes of width  $h = 1$ , while  $O_{hv}$  also includes  $h = 2$  stripes.

In this way, as stated in the STD method, both observables indicate that the  $h_1$ -TL transition is continuous and the critical temperature is  $T_c = 0.254(1)$ , where the error bars were estimated using the closest temperatures that present the smallest deviations from Eq. (6) (not shown). This result is confirmed by the time evolution of the susceptibilities that also present a power-law behavior according to Eq. (7) at the same temperature.

In order to determine the critical exponents, the Binder cumulant and the logarithmic derivative of the  $O_{hv_1}$  with respect to the reduced temperature were obtained. These observables as well as  $O_{hv_1}$  and  $O_{hv_1}^2$  were fitted with the STD equations. The STD exponents are listed in Table I and shown in Fig. 4. From the STD exponents, the critical exponents of the  $h_1$ -TL phase transition at  $\delta = 1.2585$  were estimated and are reported in both Table II and Fig. 5. Notice that the exponents  $\gamma/\nu z$  and  $\gamma/\nu$  determined from both initial conditions are in good agreement. It is worth mentioning that the critical exponents obtained from the evolution of  $O_{hv}$  and its moments were also calculated and differ from the previously calculated ones by a number smaller than 5%, except for the value of  $z$ , which differs by 10%.

The scenario is completely different if the system is started from the OC with  $h_2$ . In this case, Fig. 3(b) shows that the evolution of  $O_{hv}$  and  $O_{hv_2}$  at  $T = 0.260$  can be well fitted by Eq. (11), as shown by the dashed lines. These fits are justified by the fact that the corresponding susceptibilities,

TABLE I. Critical temperatures and STD exponents corresponding to the continuous transition lines  $h_1$ -TL and  $h_2$ -TL. The upper part reports the results for the  $h_1$ -TL phase transition using  $O_{hv_1}$  as the order parameter, while the lower part corresponds to  $h_2$ -TL and  $O_{hv}$ . The initial conditions for  $T_c$  and  $\gamma/\nu z$  are also indicated.

$\delta$	$T_c$ (DC)	$T_c$ (OC)	$\gamma/\nu z$ (DC)	$\gamma/\nu z$ (OC)	$d/z$	$1/\nu z$	$\beta/\nu z$
1.23	0.286(1)	0.285(1)	0.785(9)	0.695(8)	0.719(8)	0.657(5)	0.0122(5)
1.25	0.265(1)	0.265(1)	0.74(1)	0.682(9)	0.696(8)	0.620(9)	0.0065(2)
1.2585	0.254(1)	0.254(1)	0.586(9)	0.565(6)	0.556(6)	0.540(6)	0.0028(1)
1.37	0.426(1)	0.428(1)	0.605(5)	0.61(1)	0.65(1)	0.520(9)	0.0186(2)
1.375	0.433(1)	0.434(1)	0.573(8)	0.587(7)	0.624(9)	0.46(1)	0.0190(5)
1.40	0.465(1)	0.465(1)	0.539(5)	0.537(5)	0.584(7)	0.494(9)	0.0222(4)
1.50	0.572(1)	0.5730(5)	0.593(6)	0.599(5)	0.680(8)	0.560(5)	0.0386(6)
1.60	0.658(1)	0.6588(3)	0.622(9)	0.636(9)	0.703(9)	0.579(5)	0.0399(4)
1.70	0.722(1)	0.724(1)	0.636(8)	0.640(9)	0.727(9)	0.575(8)	0.0394(4)
1.80	0.769(1)	0.7965(5)	0.641(4)	0.65(1)	0.718(9)	0.567(9)	0.0299(5)
1.90	0.795(1)	0.795(1)	0.720(5)	0.591(8)	0.620(9)	0.50(1)	0.0180(5)

which are shown in the inset, exhibit the power-law evolution predicted by Eq. (12). This result, in addition to those displayed in Fig. 2(a), allows us to conclude that the transition  $h_2$ -TL is of first order, so the temperatures  $T = 0.260(2)$  and  $T = 0.226(6)$  can be related to the spinodal points of the phases  $h_2$  and TL, respectively. Therefore, in view of the exposed results for  $\delta = 1.2585$  at  $T_c = 0.254(1)$ , a critical phase corresponding to the transition  $h_1$ -TL coexists with the  $h_2$  phase.

### B. Phase transitions and multicritical behavior in the neighborhood of $\delta = 1.2585$

In order to avoid the possible influence of the development of domains corresponding to unstable phases during the nonequilibrium measurements, i.e., the  $h_2$  domains within the region where  $h_1$  is the stable phase and vice versa, the above-described procedure was applied in the neighborhood of  $\delta = 1.2585$ . The obtained results for the cases  $\delta = 1.25$  and

$\delta = 1.23$  indicate that the phase transition is continuous. Both the critical temperature and STD exponents of  $O_{hv_1}$  as well as its moments are reported in Table I, and the calculated critical exponents are summarized in Table II. As can be inferred from both Tables I and II,  $\gamma/\nu z$  and  $\gamma/\nu$  determined from both initial conditions present a relatively good agreement. Figure 6 shows the excellent agreement between the critical temperatures and those reported in Refs. [5,6].

With the aim of determining the value of  $\delta$  where the influence of unstable  $h_2$  domains on the critical behavior becomes negligible, the same measurements were performed using  $O_{hv}$  and its moments. The obtained critical temperatures are in agreement with those reported in Table I. This is illustrated in Fig. 7(a), where  $O_{hv}$ ,  $O_{hv_1}$ , and their susceptibilities exhibit a power-law behavior at  $T = 0.285(1)$  for the initial OC. A similar situation is found when the system is started from the DC [see Fig. 7(b)]. On the other hand, Fig. 8 shows that the difference between the critical exponents, obtained by considering both  $O_{hv_1}$  and  $O_{hv}$ , becomes less important when  $\delta$  is decreased. Furthermore, for  $\delta = 1.23$  both sets of critical exponents are in excellent agreement within the error bars.

TABLE II. Critical exponents calculated from the STD exponents listed in Table I. The upper and lower parts correspond to  $h_1$ -TL and  $h_2$ -TL phase transition lines, respectively. The initial condition for  $\gamma/\nu$  is also indicated. The exponent  $\gamma/\nu$  (DC) was estimated by using the exponent  $z$  obtained from the initial OC, which is listed in the fourth column. More details are given in the text.

$\delta$	$\beta$	$\gamma$	$z$	$\nu$	$\gamma/\nu$ (DC)	$\gamma/\nu$ (OC)
1.23	0.0186(8)	1.06(1)	2.78(3)	0.547(7)	2.18(3)	1.93(4)
1.25	0.0105(4)	1.10(2)	2.87(4)	0.56(1)	2.12(4)	1.96(5)
1.2585	0.0052(2)	1.05(2)	3.60(4)	0.515(8)	2.11(4)	2.03(4)
1.37	0.036(1)	1.17(3)	3.08(5)	0.63(1)	1.94(4)	1.88(4)
1.375	0.041(1)	1.28(3)	3.21(5)	0.68(2)	1.86(3)	1.88(4)
1.40	0.045(1)	1.09(2)	3.42(4)	0.59(1)	1.84(4)	1.84(4)
1.50	0.069(1)	1.07(1)	2.94(3)	0.607(9)	1.85(3)	1.76(3)
1.60	0.069(1)	1.10(2)	2.84(4)	0.607(9)	1.74(3)	1.81(3)
1.70	0.069(1)	1.11(2)	2.75(3)	0.63(1)	1.77(3)	1.76(3)
1.80	0.053(1)	1.14(3)	2.79(3)	0.63(1)	1.75(3)	1.81(4)
1.90	0.036(1)	1.18(3)	3.23(5)	0.62(2)	1.79(3)	1.91(4)

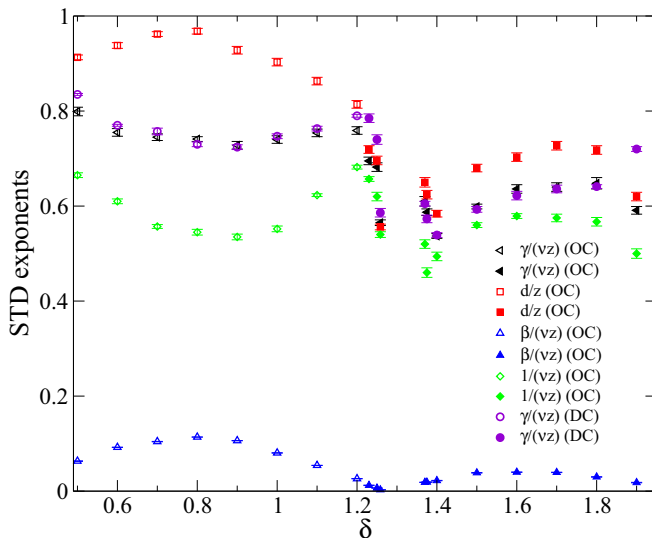


FIG. 4. STD critical exponents versus  $\delta$  obtained for both initial conditions (OC and DC) as indicated. The open symbols correspond to previously reported data in Ref. [16]. More details are given in the text.

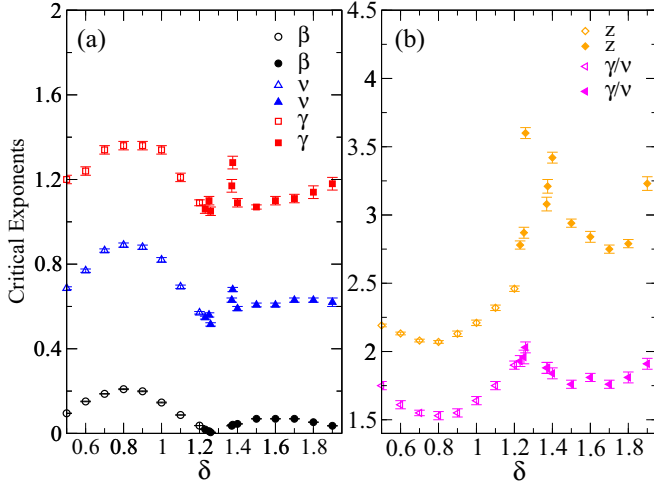


FIG. 5. Critical exponents versus  $\delta$  obtained from initial OC. The open symbols correspond to previously reported data in Ref. [16]. More details are given in the text.

These findings were also verified for  $\delta = 1.20$  by comparing the results obtained using  $O_{hv_1}$  with those reported in Ref. [16], where only  $O_{hv}$  was employed. The described results allow us to conclude that the continuous phase transition line between  $h_1$  and TL extends up to  $\delta = 1.2585$  (see Table I and Fig. 6). Furthermore, for  $\delta \leq 1.23$ ,  $O_{hv}$  is suitable to characterize this phase transition by means of the STD method.

However, for  $1.2585 < \delta \leq 1.36$ , where the  $h_2$ -TL transition takes place, the obtained results are consistent with a weak first-order phase transition (see Table III and Fig. 6). As can be observed in the inset of Fig. 6, the strength  $T_{up} - T_{down}$  takes its largest value at  $\delta = 1.2585$  and decreases up to zero

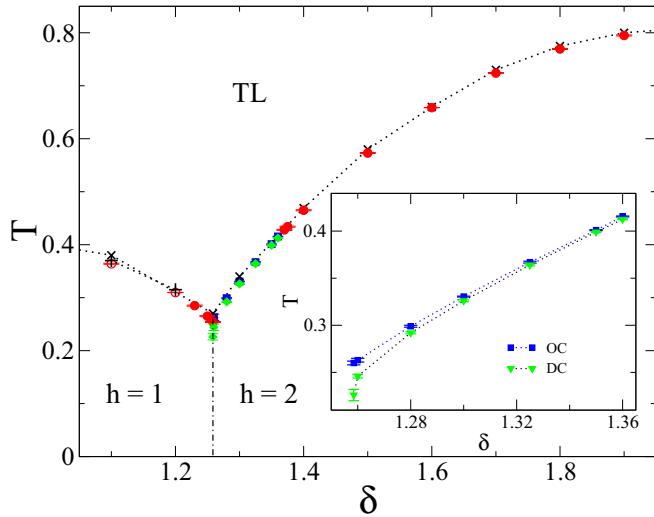


FIG. 6. Phase diagram in the  $T$ - $\delta$  plane. Open circles are from Ref. [16], crosses are from [6], and pluses were taken from Ref. [15]. Solid symbols correspond to the data obtained in the present work; circles denote the critical temperatures, while the squares and diamonds are the spinodal temperatures  $T_{up}$  and  $T_{down}$ , respectively. Dotted lines are to guide the eye, and the dashed line represents the first-order phase transition  $h_1$ - $h_2$  line that was taken from Ref. [6]. The inset shows the interval  $1.2585 \leq \delta \leq 1.36$  in more detail.

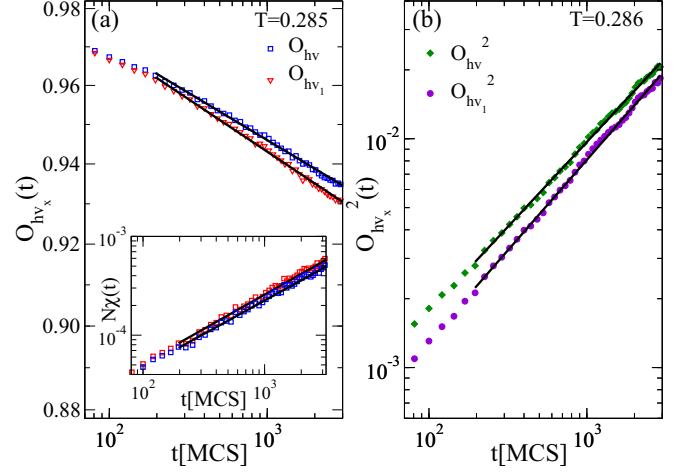


FIG. 7. Dynamic evolution of the system at  $\delta = 1.23$ : (a)  $O_{hv}$  and  $O_{hv_1}$  at  $T = 0.285$  from the ordered initial condition (OC). The inset shows the corresponding susceptibilities. (b)  $O_{hv}^2$  and  $O_{hv_1}^2$  at  $T = 0.286$  when the system is started from the DC. The solid lines represent the power-law fit by means of STD equations (6) and (7) in (a) and (10) in (b). More details are given in the text.

at  $\delta = 1.37$  (see also Table III). In addition, the value of the order parameter at the spinodals of the  $h_2$  phase ( $O_p^{sp}$ ) goes to zero with  $\delta$ . It is worth mentioning that for  $\delta > 1.26$ , the spinodal temperatures as well as  $O_p^{sp}$  obtained by using  $O_{hv}$  are in agreement with those corresponding to  $O_{hv_2}$ . This indicates that the influence on the dynamics of unstable  $h_1$  domains can be disregarded. The described results give clear evidence of the existence of a tricritical point within the interval  $1.36 < \delta \leq 1.37$  and also confirm the first-order character of the  $h_2$ -TL phase transition for  $\delta = 1.2585$ .

### C. Critical behavior on the $h_2$ -TL transition line

In this section, the research is extended to the interval  $1.37 \leq \delta \leq 1.9$ . In order to apply the STD method and based on the conclusions of the previous sections,  $O_{hv}$  was used

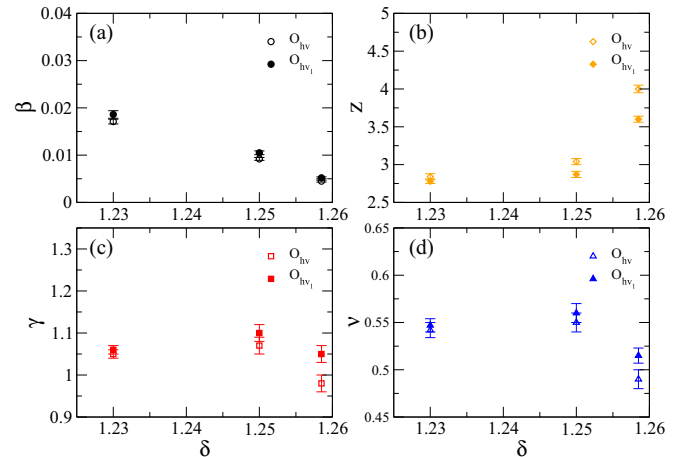


FIG. 8. Estimation of the critical exponents obtained by using STD equations and taking  $O_{hv}$  as the order parameter: (a)  $\beta$ , (b)  $z$ , (c)  $\gamma$ , and (d)  $\nu$  as a function of  $\delta$ . The results corresponding to  $O_{hv_1}$  are also included.

TABLE III. Pseudocritical temperatures  $T_{\text{down}}$  and  $T_{\text{up}}$  corresponding to spinodal points of the TL and  $h_2$  metastable phases, respectively. The fourth column reports the value of the order parameter at the spinodal of  $h_2$  phase, and the fifth column indicates the order parameter used. The initial conditions are also included.

$\delta$	$T_{\text{down}}$ (DC)	$T_{\text{up}}$ (OC)	$O_p^{sp}$ (OC)	$O_p$
1.2585	0.226(6)	0.260(2)	0.972(2)	$O_{hv_2}$
1.26	0.244(2)	0.263(2)	0.960(4)	$O_{hv_2}$
1.28	0.292(2)	0.299(1)	0.918(8)	$O_{hv}$
1.30	0.326(1)	0.3305(5)	0.89(1)	$O_{hv}$
1.325	0.364(1)	0.367(1)	0.82(1)	$O_{hv}$
1.35	0.3990(5)	0.4010(5)	0.757(5)	$O_{hv}$
1.36	0.4125(5)	0.4155(5)	0.662(5)	$O_{hv}$

as the order parameter. For each  $\delta$  value investigated and for both initial conditions, the STD observables showed a power-law behavior at the same temperature, within the error bars, indicating a continuous phase transition. The obtained temperatures are listed in the lower part of Table I. Figure 6 shows that these transition temperatures are in excellent agreement with those reported in Ref. [6]. Notice that this work suggested a first-order transition line; however, the limitations imposed by the long equilibration times and the small system sizes in the Monte Carlo studies did not lead to completely reliable conclusions. In fact, they also predicted a first-order phase transition for the  $h_1$ -TL line in the range  $1 \leq \delta \leq 1.2$ , and more recently, it was demonstrated that this line is continuous [15,16]. The continuous character determined in the present case is supported by the fit of the  $O_{hv}$  evolution with Eq. (11) that gives values  $O_{hv}^{sp} = 0$  over the whole studied  $\delta$  interval. Moreover, there is good agreement between the estimations of exponent  $\gamma/\nu z$  from both initial conditions, except for the case of  $\delta = 1.9$ , where the difference is of the order of 16%. The last difference could be related to the proximity of the nematic phase that was detected for  $\delta = 2$  [6].

The STD exponents obtained by means of the fit of the corresponding observables are listed in the lower part of Table I and are shown in Fig. 4. From these values, the critical exponents were estimated and are reported in both Table II and Fig. 5. For the sake of comparison, Figs. 4 and 5 also include the exponents corresponding to the  $h_1$ -TL transition line. As can be observed in Fig. 5(a), the static exponents,  $\beta, \gamma$ , and  $\nu$ , show a weak dependence on  $\delta$  except near the zone where the tricritical point is expected to be. Furthermore, these exponents indicate that the transition  $h_2$ -TL does not belong to the Ising universality class. On the other hand, the dynamic exponent  $z$  presents a minimum value for  $\delta = 1.7$  but always remains higher than the value corresponding to the bidimensional Ising model, i.e.,  $z = 2.1667(5)$  [22]. The last result is indicative of the slow critical dynamic behavior of the model, which is enhanced in the neighborhood of the tricritical point. A similar behavior is observed for  $z$  in the case  $h_1$ -TL close to  $\delta = 1.2585$  in Fig. 5.

#### IV. CONCLUSIONS

The phase diagram of the ferromagnetic Ising model with dipole interactions has been the object of a long-standing

controversy about the order of the high-temperature phase transitions and the possible existence of multicritical points. In the present work, the short-time dynamics method was applied to determine the nature of the transitions between the ordered stripe of width  $h = n$  ( $h_n, n = 1, 2$ ) and tetragonal liquid TL phases in the interval  $1.23 \leq \delta \leq 1.9$ .

In order to study the dynamic behavior at the point where the  $h_1$ -TL,  $h_2$ -TL, and  $h_1$ - $h_2$  transition lines meet, which corresponds to  $\delta = 1.2585$ , it was necessary to define two variants of the orientational order parameter  $O_{hv}$ . These variants, denoted as  $O_{hv_1}$  and  $O_{hv_2}$ , are capable of distinguishing an ordered stripe phase with the specific widths  $h = 1$  and  $h = 2$ , respectively. The dynamic evolution of the observables  $O_{hv_1}, O_{hv_2}$  and their moments allowed us to conclude that the  $h_1$ -TL phase transition is continuous, while the  $h_2$ -TL one presented a weak first-order character. As a consequence, at this point the critical phase corresponding to the transition  $h_1$ -TL coexists with the  $h_2$  phase. So this point must not be considered a triple point due to the fact that the three involved phases do not coexist; that is, a continuous transition line meets two first order ones. Moreover, it cannot be classified as tricritical because if it were so, all the phases would become critical. It is important to remark that, as expected, the dynamic behavior of  $O_{hv_1}$  and  $O_{hv_2}$  matched that corresponding to  $O_{hv}$  for  $\delta \leq 1.23$  and  $\delta > 1.26$ , respectively, i.e., when  $\delta$  is moved away from the  $h_1$ - $h_2$  transition line.

Furthermore, the results obtained for  $\delta < 1.2585$  allow us to conclude that the continuous  $h_1$ -TL phase transition line extends up to  $\delta = 1.2585$ . The critical exponents were determined from the STD exponents, including those corresponding to  $\delta = 1.2585$ . It was found that they depend on  $\delta$  and do not belong to the Ising universality class in any case reported. On the other hand, for  $1.2585 < \delta \leq 1.36$  the behavior of the STD observables was consistent with a weak first-order phase transition, whose strength decreases up to zero at  $\delta = 1.37$ . This result confirms the first-order character of the  $h_2$ -TL transition at  $\delta = 1.2585$  and suggests the existence of a tricritical point within the interval  $1.36 < \delta \leq 1.37$ . Finally, for  $1.37 \leq \delta \leq 1.9$  the  $h_2$ -TL transition line was found to be continuous, and consequently, the complete set of the critical exponents was obtained. As in the case of  $h_1$ -TL, the critical exponents varied with each value of  $\delta$  investigated.

It is important to remark that in this work the STD technique was successfully applied to study a point where three transition lines meet and more than two phases are present, i.e., in the case  $\delta = 1.2585$ . With this aim, it was necessary to define new order parameters that take into account the specific structure of the stripe-ordered phase. Moreover, in view of the obtained results, STD is expected to be useful to determine the nature of the phase transitions exhibited by the Ising model with dipolar interactions for larger values of  $\delta$ , which remains under discussion.

#### ACKNOWLEDGMENT

This work was supported by CONICET (PIP0143) and UNLP (X11/637), Argentina. We thank UnCaFiQT (SNCAD) for computational resources.

- [1] A. B. MacIsaac, J. P. Whitehead, M. C. Robinson, and K. De'Bell, *Phys. Rev. B* **51**, 16033 (1995).
- [2] A. B. MacIsaac, J. P. Whitehead, K. De'Bell, and K. S. Narayanan, *Phys. Rev. B* **46**, 6387 (1992).
- [3] M. B. Taylor and B. L. Gyorffy, *J. Phys. Condens. Matter* **5**, 4527 (1993).
- [4] E. Rastelli, S. Regina, and A. Tassi, *Phys. Rev. B* **73**, 144418 (2006).
- [5] E. Rastelli, S. Regina, and A. Tassi, *Phys. Rev. B* **76**, 054438 (2007).
- [6] S. A. Pighín and S. A. Cannas, *Phys. Rev. B* **75**, 224433 (2007).
- [7] L. G. Rizzi and N. A. Alves, *Phys. B (Amsterdam, Neth.)* **405**, 1571 (2010).
- [8] K. De'Bell, A. B. MacIsaac, and J. P. Whitehead, *Rev. Mod. Phys.* **72**, 225 (2000).
- [9] O. Portmann, A. Vaterlaus, and D. Pescia, *Nature (London)* **422**, 701 (2003).
- [10] O. Portmann, A. Vaterlaus, and D. Pescia, *Phys. Rev. Lett.* **96**, 047212 (2006).
- [11] N. Bergeard, S. Schaffert, V. López-Flores, N. Jaouen, J. Geilhufe, C. M. Günther, M. Schneider, C. Graves, T. Wang, B. Wu, A. Scherz, C. Baumier, R. Delaunay, F. Fortuna, M. Tortarolo, B. Tudu, O. Krupin, M. P. Minitti, J. Robinson, W. F. Schlotter, J. J. Turner, J. Lüning, S. Eisebitt, and C. Boeglin, *Phys. Rev. B* **91**, 054416 (2015).
- [12] P. M. Gleiser, F. A. Tamarit, and S. A. Cannas, *Phys. D (Amsterdam, Neth.)* **168**, 73 (2002).
- [13] P. M. Gleiser, F. A. Tamarit, S. A. Cannas, and M. A. Montemurro, *Phys. Rev. B* **68**, 134401 (2003).
- [14] I. Booth, A. B. MacIsaac, J. P. Whitehead, and K. De'Bell, *Phys. Rev. Lett.* **75**, 950 (1995).
- [15] J. S. M. Fonseca, L. G. Rizzi, and N. A. Alves, *Phys. Rev. E* **86**, 011103 (2012).
- [16] C. M. Horowitz, M. A. Bab, M. Mazzini, M. L. Rubio Puzzo, and G. P. Saracco, *Phys. Rev. E* **92**, 042127 (2015).
- [17] E. V. Albano, M. A. Bab, G. Baglietto, R. A. Borzi, T. S. Grigera, E. S. Loscar, D. E. Rodríguez, M. L. Rubio Puzzo, and G. P. Saracco, *Rep. Prog. Phys.* **74**, 026501 (2011).
- [18] D. E. Rodríguez, M. A. Bab, and E. V. Albano, *J. Stat. Mech.* (2011) P09007.
- [19] E. S. Loscar, E. E. Ferrero, T. S. Grigera, and S. A. Cannas, *J. Chem. Phys.* **131**, 024120 (2009).
- [20] R. Rürger and R. Valentí, *Phys. Rev. B* **86**, 024431 (2012).
- [21] P. P. Ewald, *Ann. Phys. (Berlin, Ger.)* **369**, 253 (1921).
- [22] M. P. Nightingale and H. W. J. Blöte, *Phys. Rev. B* **62**, 1089 (2000).